EDMX Research Day 2026

3rd February 2026, 11:00 – 18:00, CO

Time	Session	Speaker – Presentation – Activity
10:30 – 11:00	**Registration & Coffee**	Mounting of posters on pinboards
11:00 – 11:20	**Welcome & Introduction**	**Prof. Esther Amstad** EDMX Program Director
11:20 - 11:40	**Talk**	**Dr Matteo Hirsch** From the Lab to the Shelf – Driving Sustainability in Food Packaging at Nestlé
11:40 – 12:00	**Pitch talks**	1-minute talks by poster presenters (Public voting for prize)
12:00 – 12:05	**Group photo**	
12:05 – 13:15	**Lunch break & Poster session 1**	Odd numbers
13:15 – 14:15	**Doctoral students talks**	**Julia Lorenzetti (501 - Materials for Energy Conversion)** Enhancing solid booster utilization in redox targeted flow batteries with non-fluorinated binders **Ray Cowen (LRM)** (SENS)2 of calcium−silicate−hydrate: Probing the atomic-level surface structure of cements **Ekaterina Poliukhina (SUNMIL)** Direct measurement of protein pair interaction potentials
14:15 – 15:30	**Coffee break & Poster session 2**	Even numbers
15:30 – 16:30	**Round table discussion with EDMX alumni**	**Dr Lorenz Hagelüken** **Dr Michele Bozzetti** **Dr Matteo Hirsch** **Dr Sophia Thiele**
16:30 – 17:00	**Prize awards & Conclusions**	**Prof. Esther Amstad** EDMX Program Director
17:00 – 18:00	**Closing apéro**	

Scientific Committee: Dr Allison Chau (SMaL), Dr Julie Gheysen (LMM), Dr Deepika Sardana (SUNMIL), Dr Morgan Barbey-Binggeli (INE), Dr Calixe Bénier (TIC), Dr Javier Castillo Seoane (LMSC), Dr Ignacio Rodriguez Barber (LMM)

Posters list (Posters marked with a * are giving pitch presentations)

Number	Name	Poster Title
1*	Abdullah Aydemir	Improving high temperature properties of Hastelloy X through microstructure engineering and oxide dispersion strengthening
2	Adam Woodhouse	ABA Triblock Copolymer Hydrogels with Bio-inspired Physical Crosslinks
3	Aleksandr Poliukhin	Electron-phonon interactions beyond DFT
4	Anna Koptelova	Protein-Based Materials from Amyloid Fibrils: Composite Films and Multilayers
5	Anna Duvakina	Static and dynamic magnetic properties of corrugated NiFe thin films patterned by DNA-self-assembled nanotemplates.
6*	Annalena Erlacher	Pressure- and temperature-driven microstructural and grain boundary evolution in alumina
7	Anthony Hoogmartens	Enhancing reprocessability of dynamic polymer composites with thermally sensitive particles and controlled particle-matrix interfaces
8	Arslan Mazitov	Lightweight, universal machine-learning model for atomistic materials simulations
9	Atreyee Acharya	Multiscale characterization of failed bioprosthetic heart valves using X-rays
10	Axel Deenen	Superconducting Diode Effect in Hollow Superconducting Helices
11	Biruktait Ayele Lemecho	Integrating CO2 Capture,Conversion to Methane in Compact Device for Mars In situ Propellant Production
12	Blanca de Miguel Martínez	Production of bio-based materials from fungal fermentation
13	Brian Ridenour	Bioinspired Design of Nano-Reinforced Granular Hydrogels
14	Bruno Ploumhans	Discretization Error Quantification in Plane-Wave Density Functional Theory
15	Buse Tatli	Influence of Glucose-Based Additives on Cellulose Nanocrystal Self-Assembly
16	Ceren Mitmit	Improving Voc in wide bandgap ACIGS solar cells
17	Claire Paetsch	First-principles thermodynamics of hydrogen absorption in binary C15 Laves phases
18	Damien Lee	Modeling the equilibrium vacancy concentration in multi-principal element alloys from first-principles
19	Deepak Somani	First-principles models of defects in alloys

20	Ding Ren	Low-Density Lipoprotein Forming Corona: Characterization and Use in Cancer Detection
21*	Disha Bandyopadhyay	Self healing polymers for reconfigurable architected structures
22	Egor Rumiantsev	Including Long-Range Interactions and Electric Response in Machine Learning Potentials
23	Ekaterina Poliukhina	Direct measurement of protein pair interaction potentials
24	Etchevers Marjorie	Factors influencing early-age properties of clinker
25	Ferdinand Posva	Supercurrent in a lateral S/F/S Josephson junction incorporating NbTiN and Ni grown by atomic layer deposition
26	Filip Koldzic	Effect of Supramolecular End Group Dynamics on Bulk Relaxation in a High Molar Mass Polyester
27	François Rivat	Moisture-Initiated Crosslinking of 3D Printed Double-Network Granular Elastomers
28	Gaëtan Denis	Electro Sinter Forging Process and Properties
29	Guoyuan Liu	Beyond DFT: delta learning on transition-metal oxides
30	Hari Priya Ravindran	Thermodynamic kinetic modelling of calcium aluminium sulphates
31	Hendrik Jansen	When Interfaces Fail: Thermal Stability and Mechanical Consequences in Metal–Ceramic Nanocomposites
32	Hien Tran Thi	Repurposing virustatic Resveratrol into a broad-spectrum virucidal with elevated non-toxicity and anti-inflammation activities
33	Jean-Baptiste Desbrest	Process windows for debondable adhesives in high performance aerospace applications
34	Jinwon Song	Thermally Drawn Stretchable Optical Fibers
35	Joao Pedro Assuncao	Squaraine dye based organic photomultiplication diodes with 220% external quantum efficiency at 1240 nm
36	Julia Lorenzetti	Enhancing Solid Booster Utilization in Redox Targeted Flow Batteries with Non-Fluorinated Binders
37	Kamila Hamulka	Effects of strain rate and c-axis orientation on microscale α-Ti compression: From kink bands to twinning
38*	Kewei Zhou	Ultrafast Dynamics of Magnetic Flux Quanta in a Superconducting Ring
39	Kyle Haas	Unassisted Water Splitting with Earth-Abundant Semiconductors
40	Lianxin Xu	Optimized silane chemical vapor deposition for robust aptamer nanopore functionalization
41*	Lorenzo Piersante	Two-step nucleation lowers energy barriers for structural transformations in metallic alloys
42	Louis Gobber	THz control of diamond NV centers
43	Luca Righetti	Quantum embedding for strongly correlated defects in PAW calculations from the algorithmic inversion method

44	Maja Lopandic	Swelling Accelerated Reduction of Disulfide-Crosslinked Tetra-PEG Networks
45	Malo Hervé	Ultrafast Magnetic Fields from THz-Driven Chiral Phonons
46	Mario Caserta	xc-functional dependence of the local screened Coulomb interaction and the dynamical Hubbard functional
47	Martina Birocco	Assessing humidity-induced fracture toughness degradation in polycrystalline alumina
48	Matteo Darra	The Effect of Cellulose Surface Chemistry on Mycelium-Cellulose Nanofiber Composites
49	Matthias Kellner	Advances in chemical shielding predictions of organic solids
50	Michele Bonacina	Superhydrophobic coatings by UV-PIPS
51	Mohammad Mobasheri	Phase transformations in recycling of waste concrete through thermal processing
52	Nataliya Paulish	Databases of Fermi surfaces and de Haas-van Alphen oscillation frequencies from first principles simulations
53	Nianduo Cai	Nanopore sensor-enabled single-molecule detection
54	Nicola Carrara	Enzyme-responsive nanofertilizer for sustainable agriculture
55*	Philipp Kroeker	Secondary Twinning and Twin–Twin Interaction Mechanisms of {11-21} deformation twins in Rhenium
56	Raphael Lemerle	Boosting Performance of Zn3P2/InP Heterojunction Solar Cells through Selective Area Epitaxy
57	Ray Cowen	(SENS)2 of calcium−silicate−hydrate: Probing the atomic-level surface structure of cements
58	Richa Rajadhyax	Structural metrics of gas diffusion electrodes used in CO2-to-CO electroreduction by FIB-SEM tomography
59	Robert Wojtaszczyk	Understanding the Contribution of Tricalcium Aluminate in the Early Strength Development of Portland Cements
60	Robin Studer	Salt Hydrate-Based Hydrogel Composite Materials for Energy Storage Applications
61	Rocio Garcia Montero	Room Temperature 3D Bioprinting of Functional Organoids
62	Samuel Bojarski	PVD/ALD Asymmetric Nanolaminates: Multilayer Libraries to Explore Thermal Stability of Cu-X Binary Alloys
63	Samuel Gatti	How to bring new battery materials to scale? Continuous production of carbon coated Na3V2(PO4)3
64	Sandor Lipcsei	Nanoindentation Of Oxide Inclusions In Iron
65	Sebastian Niedermeyer	Analysis of Axial Hydrogen Diffusion and Hydride Precipitation in Zirconium Alloy Nuclear Fuel Claddings
66	Shixuan Shan	Variable Charge State, Magnetic Excitations, and Kondo-Effect of Sm/graphene/Ir(111)
67	Simone Cigagna	Forces within the dynamical Hubbard functional framework

68	Sneha Cheriyamparambil	Protein Mimics by Ring-Opening Polymerization of Amino Acid N-Carboxyanhydrides
69*	Sudharsan Rathna Kumar	Quantifying the CO2 Absorbed by Cement-Based Materials over their Lifetime
70	Suqiu Jiang	A Surface-Initiated Polymerization Strategy for the Controlled Synthesis of PDMS Brushes
71	Thanh Thi Ha Le	Glyoxylic Acid (GA)-Lignin as Paper Barrier Coatings for Food Packaging Applications
72	Timo Reents	Score-based diffusion models for accurate crystal-structure inpainting and reconstruction of hydrogen positions
73	Tushar Thakur	Novel fast Li-ion conductors for solid-state electrolytes from first-principles
74	Tyler Benkley	Numerical Simulations of an Additive Manufacturing Process
75*	Vahid Charkhesht	Graphene-based Supercapacitors: Bridging Energy and Power
76	William Le Bas	Explaining Interlayer Bonding of Additively Manufactured Aluminium through Fractography
77	Yameng Lou	The Effect of Ligands Randomness and Flexibility on Super-selective Multivalent Interactions
78	Yann Muller	First-Principles Thermodynamics of Multicomponent Alloys
79	Yuki Hayashi	Effect of Carbon Source Diversity on Mycelium's Structure and Mechanical Properties
80	Zoubeir Saraw	Mussel byssus-inspired spinning of ionically crosslinked fibers
81	Umut Altuntas	Microscopic Measurement of the Local Deformation Field for Soft Brittle Materials Under Cyclic Loading
82	Corentin Foucher	Investigation of Impact Mitigation Strategies: Biomimicking the Muskox Skull
83	Marie-Gabrielle Ameres	Advanced Operando Vibrational Spectroscopy to Resolve Active-Site Structures in Vanadium-based Catalysts
84	Yan Meng	Chalcogenide Glass Nanowire Array by Thermal Drawing for Strong Optical Resonance
85	Andrea Pintus	Self-consistent spectral functional approach for correlated solid
86	Sandra Saade	Exploring the design space of physically-constrained machine learning models for Hamiltonian derived properties
87	Chiara Ongaro	2-step processes for wide bandgap perovskite absorbers
88	Pierpaolo Ranieri	Mapping ferroelectric fields by precession assisted pixelated differential phase contrast
89	Vishal Kumar	Does pulsed-electron beam illumination reduce beam damage for imaging biological specimens?

Enhancing Solid Booster Utilization in Redox Targeted Flow Batteries with Non-Fluorinated Binders

Julia Lorenzetti[1,2], Paweł P. Ziemiański[1], Cédric Kupferschmid[1], David Reber[1]

[1]*Empa, Swiss Federal Laboratories for Materials Science and Technology, Dübendorf, Switzerland*

[2]*EPFL, School of Engineering, Institute of Materials, Lausanne, Switzerland*

The low energy density of redox flow batteries can be mitigated by incorporating solid capacity boosters in the electrolyte tanks. A redox mediator in solution (electrolyte) is charged/discharged in the electrochemical cell and pumped into the tank where it reacts chemically with the booster (solid electrode material). If this reaction is reasonably fast, the energy density of flow batteries can be improved manyfold due to the much higher charge storage capacity of solid electrode materials compared to dissolved active species. For example, lithium iron phosphate (LFP) was shown to be a suitable solid booster in combination with ferricyanide as a redox mediator.[1] Until now, polyvinylidene fluoride (PVDF) has been used as a binder in the manufacturing of booster pellets.[2, 3] Amid growing concerns and tightening regulations surrounding PFAS compounds, we extruded LFP pellets with the non-fluorinated binder polycaprolactone (PCL) and screened their reaction rates using on-line UV–Vis spectroscopy. By replacing PVDF with PCL, the reaction rate between LFP and ferricyanide increased from 19% to 55% of LFP converted per hour. The increased rate can be explained by
the lower hydrophobicity of PCL, determined by contact angle analysis. Non-fluorinated LFP boosters also exhibited improved capacity utilization during charge–discharge cycling in a symmetric flow battery, reaching nearly 100% at 1 mA cm^{-2} compared to 85% for PVDF at the same current density. We demonstrate that replacing PVDF with non-fluorinated binders in solid booster composites offers a simple and immediately applicable strategy to improve both the efficiency and sustainability of aqueous RTFBs.

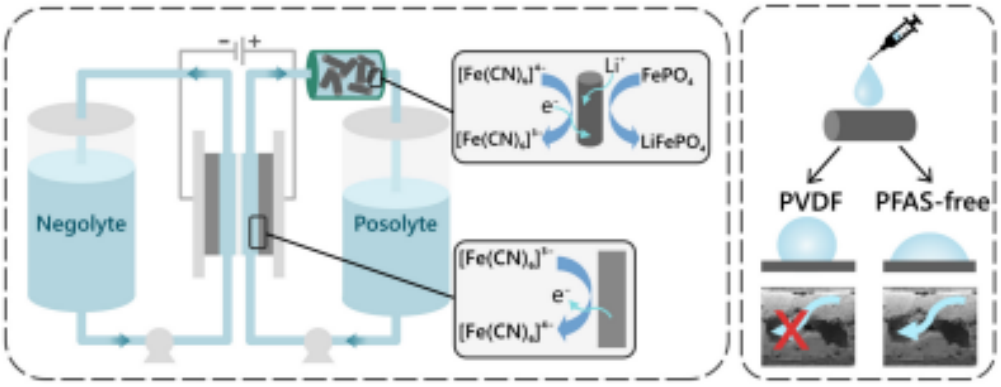

Fig. 1: *Schematics of a redox targeted flow battery (left) and contact angle of water on a booster composite depending on binder (right).*[4]

References

(1) Vivo-Vilches, J. F. *et al*. J. Power Sources **2021**, *488*, 229387. DOI: 10.1016/j.jpowsour.2020.229387.
(2) Lotenberg, T. *et al*. J. Power Sources **2024**, *602*, 234290. DOI: 10.1016/j.jpowsour.2020.229387.
(3) Marin-Tajadura, G. *et al*. Adv. En. Mater. **2025**, *15*(19). DOI: 10.1002/aenm.202404501.
(4) Lorenzetti, J. *et al*. submitted.

$(SENS)^2$ of calcium−silicate−hydrate: Probing the atomic-level surface structure of cements

X. Ray Cowen,[1,2] Tristan Georges,[1] Karen Scrivener,[2] Lyndon Emsley[1]

[1]*Laboratory of Magnetic Resonance, Institut des Sciences et Ingéniere Chemiques*
[2]*Laboratory of Construction Materials, Institut des Matériaux*

Cements are a major source of anthropogenic CO_2 emissions, driving a need to develop alternatives to carbon-intensive components. These alternatives, however, tend to weaken the primary binding phase, calcium silicate hydrate (C–S–H). A detailed understanding of the surface structure of C–S–H at the atomic-level, in particular, is crucial in developing insights to control the hydration reaction as well as mechanical and chemical properties.

Nuclear magnetic resonance (NMR) spectroscopy has proven to be a powerful tool in the atomic-level study of C–S–H; from its first use in the 1980s,[1] to the observation of the later stages of the hydration reaction[2] or the determination of the bulk structure of C−S−H.[3] However, while the bulk structure of C–S–H is well-characterized at the atomic level, direct experimental probes of the surface structure remain elusive. The extremely thin nature of C–S–H (~5 nm), and the ubiquity of hydrogen atoms throughout the structure, makes the application of even traditional surface-selective NMR techniques challenging.

Here, for the first time, we experimentally differentiate the surface structure from the bulk using new surface-enhanced NMR methods. With the isotopic selectivity of NMR and selective deuteration near the surface of the C–S–H, we are able to isolate NMR signals from silicate units originating at exclusively the surface of the material, thus allowing for characterization of the surface structure and comparison to the bulk. This breakthrough allows for analysis of the surface of C–S–H and its variants to uncover connections between atomic structure and macro-scale properties, a crucial step in the development of low-carbon cements

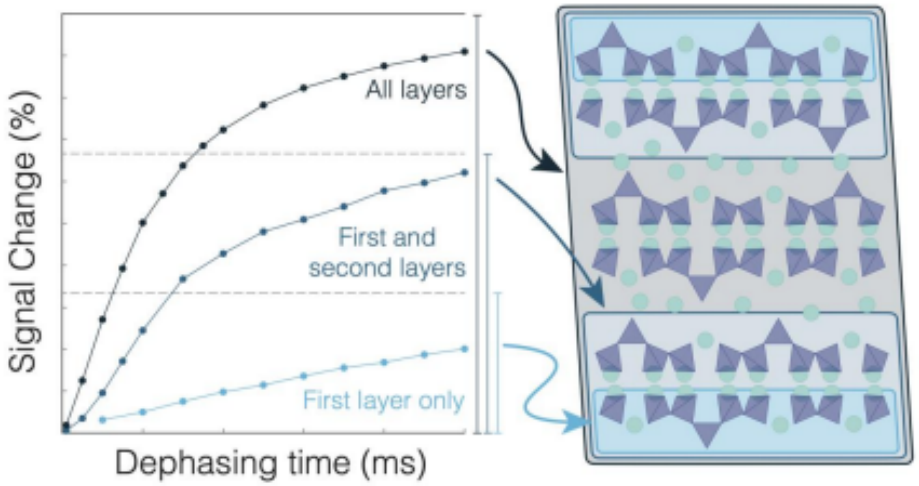

References
[1] *Cem. Concr. Res.* **1982**, *12,* 333-339.
[2] *Cem. Concr. Res.* **2004**, *34,* 857-868.
[3] *J. Phys. Chem. C* **2017**, *121* (32), 17188-17196.

Direct measurement of protein pair interaction potentials

E. Poliukhina,[1] Q. K. Ong,[1] and F. Stellacci[1,2]

[1]Institute of Materials, Ecole Polytechnique Fédérale de Lausanne (EPFL), Lausanne, Switzerland [2]Bioengineering Institute, Ecole Polytechnique Fédérale de Lausanne (EPFL), Lausanne, Switzerland e-mail: ekaterina.poliukhina@epfl.ch

A direct and unambiguous method for obtaining protein pair interaction potentials (PIPs) does not currently exist. All available approaches require solving an inverse problem, which can allow for multiple solutions. Here, we report a straightforward method to obtain the PIP directly from experimentally determined three-dimensional protein spatial distributions. Our approach builds on improvements to a recently developed cryogenic electron tomography (cryo-ET) framework for determining the potential of mean force for nanoparticles [1]. For protein PIPs, we find strong agreement between the structure factor computed from cryo-ET positions and that obtained by small-angle X-ray scattering (SAXS) of protein solutions. We further introduce a novel sub-volume method to compute Kirkwood–Buff integrals and show that second virial coefficients derived from cryo-ET tomograms closely match those measured by analytical ultracentrifugation. Together, these results validate our approach for deriving the PIP and indicate that the vitrified state faithfully reflects the solution state. We demonstrate the generality of this method across several small proteins with distinct structures and molecular weights under varied experimental conditions, including changes in salt concentration, temperature, and pH. As an example, we show that adding amino acids can shift the PIP from a net-attractive to a fully repulsive regime, consistent with our recently published theoretical framework describing amino-acid-driven stabilization mechanisms [2]. Finally, we will present a novel extension of the method to capture the role of anisotropic protein interactions.

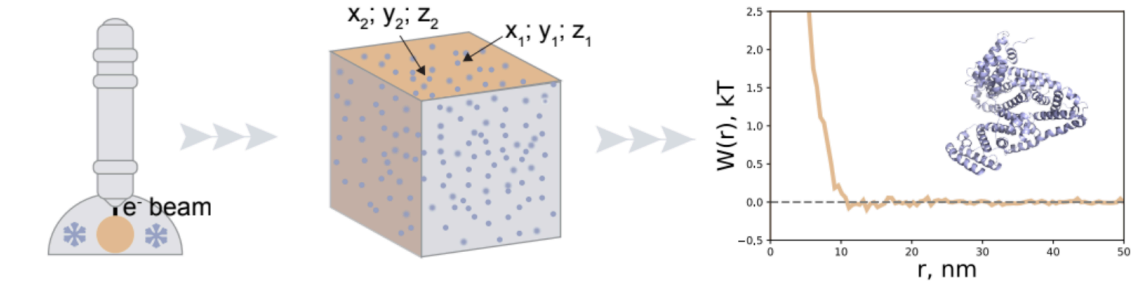

References

[1] Q. Ong, T. Mao, N. Iranpour Anaraki, Ł. Richter, C. Malinverni, X. Xu, F. Olgiati, P. H. J. Silva, A. Murello, A. Neels, D. Demurtas, S. Shimizu, F. Stellacci. *Mater. Horiz.* (2022) *9* (1), 303–311.

[2] Mao, T., Xu, X., Winkler, P.M. *et al.* Stabilizing effect of amino acids on protein and colloidal dispersions. *Nature* (2025) 645, 915–921.